Structural and optical properties of polyaniline/nickel ferrite nanocomposites

Arti I. Nandapure[1*], Subhash B. Kondawar[2], Bharti I. Nandapure[3], Manish M. Choudhari[4]

[1]*Department of Physics, B. D. College of Engineering, Sewagram, Wardha 442001, India*
[2]*Department of Physics, Rashtrasant Tukadoji Maharaj Nagpur University, Nagpur 440033, India*
[3]*Department of Physics, D. R. B. Sindhu Mahavidyalaya, Nagpur 440017, India*
[4]*Department of Civil Engineering, S. D. College of Engineering, Wardha 442001, India*

[*]Corresponding author: Tel: (+91) 9665063380; E-mail: artibd.2008@rediffmail.com

Abstract

Polyaniline/ferrite nanocomposites have attracted increasing attention because they offer the possibility of a new generation of nanostructure materials with advanced applications like electromagnetic interference shielding, rechargeable batteries, corrosion devices due to their flexibility, inexpensive and easy of synthesis. Polyaniline (PANI) containing MFe_2O_4 were prepared by in-situ polymerization of aniline in aqueous solution (Where M-represent divalent metal cation, $M^{2+} = Ni^{2+}$). PANI reduces the agglomeration of nanosized nickel ferrite ($NiFe_2O_4$) particles which is good for the stabilization of nanoparticles. The investigation of structural, morphological and optical properties was carried out for the synthesized $PANI/NiFe_2O_4$ nanocomposites using X-ray diffraction (XRD), Transmission electron microscopy (TEM) and Ultraviolet visible spectrophotometer (UV-Vis). XRD revealed that the structure of $NiFe_2O_4$ nanoparticles is spinel with space group Fd3m and crystallite size 14 nm. Lattice parameter was found to increases with $NiFe_2O_4$ concentration in PANI and this may be due to the larger ionic radius of the Ni^{2+} ion. XRD pattern of $PANI/NiFe_2O_4$ nanocomposites at different ferrite molar percent are just the superposition of those of polyaniline and ferrite nanoparticles. Transmission electron microscopy of $PANI/NiFe_2O_4$ nanocomposites show increase in particle size over pure a $NiFe_2O_4$ nanoparticles which is relevant with XRD results. UV-Visible absorption spectroscopy of $PANI/NiFe_2O_4$ nanocomposites shows two absorption bands in range of 300-350 nm and 600-650 nm which reflects interaction of ferrite nanoparticles with PANI. Copyright © 2017 VBRI Press.

Keywords: Polyaniline, nickel ferrite, nanocomposite, in-situ polymerization, optical band gap.

Introduction

Ferrospinel compounds are a very important group of magnetic materials due to their extensive use in a wide range of applications from low to high permeability devices including electronics, ferrofluid, magnetic drug delivery microwave devices and high-density information storage devices. They have the general formula of MFe_2O_4 (where M: Co, Ni etc.) in which unit cell contains 32 O-atoms in a cube close packing with 8 tetrahedral and 16 octahedral occupied sites. Among the various ferrites, nickel ferrite has been extensively used in electronic devices because of their large permeability at high frequency, remarkably high electrical resistivity, mechanical hardness, chemical stability, and cost-effectiveness. Stoichiometric $NiFe_2O_4$ consider as n-type semiconductor Also, it exhibits unusual physical and chemical properties when its size is reduced to nanosize. Nickel ferrite ($NiFe_2O_4$) is an inverse spinel in which half of the ferric ions fill the tetrahedral sites (A-sites) and the rest occupy the octahedral sites (B-sites) [1-4].

In recent years, the development of inorganic/polymer hybrid materials on nanometer scale have been receiving significant attention due to a wide range of potential applications in optoelectronic devices and in field effect transistors. The inorganic fillers at nanoscale exhibit high surface to volume ratio and thus expected to modify drastically the electrical, optical and dielectric properties of polymer. In general, the synthesis of hybrid of polymer/inorganic material has the goal of obtaining a new composite material having synergetic or complementary behaviors between the polymer and inorganic material. Conducting polymers are a new group of synthetic polymers which combines the chemical and mechanical properties of polymers with the electronic properties of metals and semiconductors [5-8]. They have extended p-conjugation with single and double-bond alteration along its chain. They behave as a semiconductor material with low charge carrier mobility and their conductivity is increased to reach the metallic range by doping with appropriate dopants. The conducting emeraldine salt form (PANI-ES) is achieved by doping with aqueous protonic or functionalized acids where protons are added to the –N= sites. This leads to an increase in the conductivity by more than ten orders of magnitude depending on the strength of the acid and the

method of processing. Polyaniline (PANI) is a most studied polymer because of its relative ease in preparation, good environmental stability and tunable conductivity. Several reports on the synthesis of composite of nanofillers like: TiO_2, CdS, Na+-montmorillonite, Pd and Au with PANI have been demonstrated [**9-13**]. Since the conducting polyaniline and inorganic semiconducting material $NiFe_2O_4$ in nanoform both are having a wide range of technological applications, we have motivated to make composite of PANI and $NiFe_2O_4$ and believed to get novel properties resulting from the molecular level interaction of these two dissimilar chemical components.

There are few reports on the synthesis, morphological, electrical and optical studies of PANI/$NiFe_2O_4$ nanocomposites. Magnetic properties of $NiFe_2O_4$ nanoparticles have been studied by K. Maaz, S. Karim, A. Mumtaz, and coworkers [**14**]. M. Khairy and M. E. Gouda, [**15**] studied Electrical and optical properties of PANI/$NiFe_2O_4$ nanocomposites. M. Patil and V. Shrivastav [**16**] reported about the removal of a MG (malachite green) dye from aqueous solution using polyaniline PANI/$NiFe_2O_4$ nanocomposites. Hence, the preparation of PANI/$NiFe_2O_4$ nanocomposites has attracted considerable interest owing to its impact on governing their ultimate performance and applications [**17-21**].

In this paper for the first time, we report systematic investigation on the effect of $NiFe_2O_4$ doping on structural, morphological and optical properties of PANI/$NiFe_2O_4$ nanocomposites. Much effort has been put into the investigation of the interaction between PANI and $NiFe_2O_4$ in order to gain a better understanding of the doping effect of $NiFe_2O_4$. The structural, morphological and optical properties of PANI/$NiFe_2O_4$ nanocomposites were investigated using XRD, TEM and UV-Vis spectroscopy. These nanocomposites have the ability to enhance their electromagnetic properties due to which such materials can be applied to ferrofluid, magnetic refrigeration, sensors, magnetic data storage, electro-magnetic resonance wave absorption, etc. We present here the preparation of PANI/$NiFe_2O_4$ nanocomposites by in-situ polymerization of aniline in the presence of Nickels nitrate as precursor using nitric acid and its characterizations [**22-24**].

Experimental

Materials/ chemicals details

Aniline monomer (distilled under reduced pressure and stored below 0^0C) (purity 98.5%), Sulphuric acid (H_2SO_4, purity 98%), Ammonium peroxydisulphate (APS, purity 99%), Sodium hydroxide (NaOH, purity 99%), Nickel nitrate ($Ni(NO_3)_2.6H_2O$, purity 99%), Ferric nitrate ($Fe(NO_3)_3.9H_2O$, purity 99%), starch ($C_6H_{10}O_5)_n$, purity 99%) were purchased from Sigma-Aldrich Fine-Chem. Ltd. and used as received without further purification. All supplementary chemicals were of analytical grade and solutions were prepared with double distilled water.

Synthesis of nanocrystalline NiFe$_2$O$_4$

$NiFe_2O_4$ nanoparticles were prepared by the simple approach of reflux method [**25**]**.** In a typical procedure, specific molar concentration of nickel nitrate and ferric nitrate as precursors were mixed in a starch solution and stirred for half an hour. Under reflux condition, NaOH was added drop by drop for 4 h to provide a net negative surface charge to the nuclei limiting their further growth and aggregation. After refluxing, the solution was kept overnight and then filtered and dried in hot air oven at 80^oC for 12 h. Dried sample was treated at different temperatures 800^oC, 900^oC, 1000^oC, 1100^oC in order to maintain the stability of compound.

Synthesis of PANI/NiFe$_2$O$_4$ nanocomposites

PANI/$NiFe_2O_4$ nanocomposites of various compositions were prepared by the method of in-situ chemical oxidation polymerization of aniline in aqueous solution of Sulfuric acid using APS as an oxidant, with different percentage of $NiFe_2O_4$ powder (10, 20, 30%) at room temperature [26-28]. Schematic formation of PANI/$NiFe_2O_4$ nanocomposites are shown in **Scheme 1**. Prepare 1M of aqueous H_2SO_4 solution. Under 1 Hr. stirrer condition, adds 0.1M of pure aniline and Ammonium peroxydisulphate to start the polymerization of aniline. 10, 20, and 30% of corresponding $NiFe_2O_4$ was added in resulting solution and sonicated for 1Hr in order to reduce the aggregation of ferrite nanoparticles. Stir the solution very well by using magnetic stirrer until a good degree of polymerization was achieved. The precipitate produced in the reaction was removed by filtration, washed repeatedly with methanol and dried under vacuum for 24 Hrs. This has led to the formation of PANI/$NiFe_2O_4$ nanocomposites. The different content of PANI/$NiFe_2O_4$ nanocomposites were abbreviated as PNF-10%, PNF-20%, PNF-30% respectively for PANI/$NiFe_2O_4$ (10%), PANI/$NiFe_2O_4$ (20%), PANI/$NiFe_2O_4$ (30%).

Characterizations

X-ray diffraction (XRD) analysis of $NiFe_2O_4$, PANI and PANI/$NiFe_2O_4$ nanocomposites were conducted on Philips PW1710 automatic X-ray diffractometer with Cu-K_α radiation ($\lambda = 1.5404$ Å), with a scanning speed of $10°\,min^{-1}$. Surface morphology of all synthesized sample were investigated by transmission electron microscopy (TEM) (Hitachi H-7000 operated at 100 kV and 30 µA). The optical absorption spectra of prepared sample were carried out using UV-1800 Shimadzu double beam UV-VIS spectrophotometer.

Results and discussion

Fig. 1(**a**) shows the XRD spectra of pure PANI and $NiFe_2O_4$ nanoparticles. XRD spectrum of PANI shows amorphous nature in partially crystalline state with two diffraction peaks at 20^0 and 26^0. The planes of Benzinoid and Quinoid rings of PANI Chain are responsible for crystalline structure [**29-32**]. XRD pattern of $NiFe_2O_4$

nanoparticles shows that main characteristic peaks which are consistence with the characteristic reflections of the Fd-3m spinel cubic structure matches well with JCPDS data 10-325 in which Ni^{2+} ions occupying the octahedral sub-lattices and Fe^{3+}ions occupying the tetrahedral sublattices. XRD spectra of $NiFe_2O_4$ showed diffraction peaks at $2\theta = 29.90^0$, 35.27^0, 36.96^0, 42.93^0, which can be indexed to (220), (311), (222) and (400) reflections. The diffraction peaks are broadened, which can be the result of grain size reduction as well as the atomic level strain introduced during the reflux process. The average crystallite size of the $NiFe_2O_4$ was found to be 14nm from the full width at half maximum reflection (311) peak in the XRD pattern using Debye Scherrer formula [**33-34**]. **Fig. 1(b)** shows the XRD spectra of PANI/$NiFe_2O_4$ nanocomposites. With the insertion of $NiFe_2O_4$ into a PANI matrix, the diffraction peaks become narrower and sharper, suggesting the increase in particle size and crystallinity. This result indicates that the crystalline sizes increase with the % of $NiFe_2O_4$ in PANI and reach the values of 22, 39 and 51 nm respectively. This might be due to the dominance of the activation energy during the $NiFe_2O_4$ nanograins growth process. Hence the particle size of PANI/$NiFe_2O_4$ nanocomposites increases with increase in content of $NiFe_2O_4$ nanoparticles in PANI [**35**].

(a)

(b)
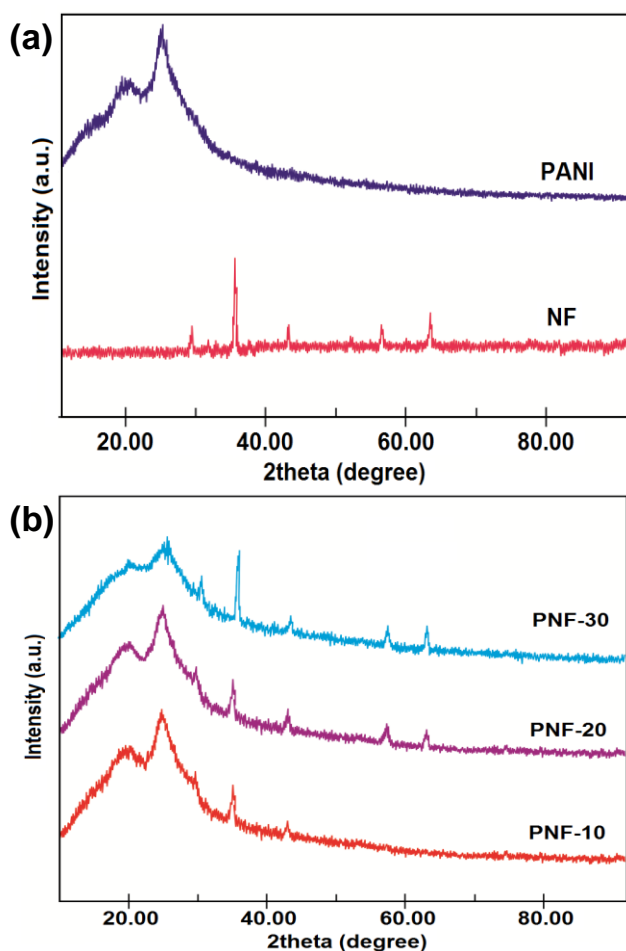
Fig. 1. (a). XRD spectra of PANI and $NiFe_2O_4$ and (b). XRD spectra of PANI/$NiFe_2O_4$ nanocomposites.

In the obtained diffraction pattern the lattice constants are found to increase from 10% to 30% as the $NiFe_2O_4$ concentration increased in polymer matrix. The increased in lattice constant with $NiFe_2O_4$ concentration may be due to the larger ionic radius of Ni^{2+} ions. The small differences in the lattice parameter sizes were observed for the all samples because Fe^{3+}ions and Ni^{2+}ions are attributed to homogeneity in spinel structure and there is a strong electrostatic force between ions. The PANI/$NiFe_2O_4$ nanocomposites (PNF-10, PNF-20, PNF-30) show crystalline peaks due to the presence of $NiFe_2O_4$ nanoparticles in these nanocomposites. The degree of crystallinity was found to increase with increasing the amount of $NiFe_2O_4$ nanoparticles in PANI.

Table 1 shows the lattice constant, volume, density and particle size for $NiFe_2O_4$ and PANI/$NiFe_2O_4$ nanocomposites. X-ray density of nanocomposites were calculated using the relation (1),

$$\rho = \frac{8M}{Na^3} \qquad (1)$$

where, M is the molecular weight, N is Avogadro's number and a is the lattice parameter respectively. The fact that the x-ray densities increase with the nanocomposites from 10 to 30% may be attributed to the result of decreasing porosity during the formation process. In PANI/$NiFe_2O_4$ nanocomposites nickel ferrite being an n-type surrounded by p-type PANI forms p-n junction in which electrons from n-type $NiFe_2O_4$ crystallites attracts holes from p-type PANI and vice versa. Due to this positive and negative ion formed across the boundary which makes depletion region. When X-ray light is exposed on such nanocomposites depletion region field polarizes the molecules provide the positive charge to PANI molecules and create some free holes on PANI molecules makes $NiFe_2O_4$ nanocomposites more conducting electrically.

Table 1. Lattice constant, volume, Density and Particle size for $NiFe_2O_4$ and PANI/$NiFe_2O_4$ nanocomposites.

Polymer	d-spacing (Å)	Lattice constant (Å)	Volume (nm^-3)	Density (g/cm^3)	Particle size (nm)
NF	2.53	8.39	590.5	5.45	14
PNF-10%	2.60	8.52	640.5	1.79	22
PNF-20%	2.68	8.68	700.2	2.61	39
PNF-30%	2.72	8.79	733.8	3.22	51

Fig. 2(a) and **2(b)** shows TEM images of pure $NiFe_2O_4$ nanoparticles and PANI/$NiFe_2O_4$ nanocomposites (30%) respectively [36]. From polygonic morphology of $NiFe_2O_4$ nanoparticles, the average particle size was observed as 30nm, whereas average particle size of PANI/$NiFe_2O_4$ nanocomposite (30%) was observed as 40nm. PANI/$NiFe_2O_4$ nanocomposite (30%) shows the confirmation of interaction between $NiFe_2O_4$ nanoparticles and PANI.
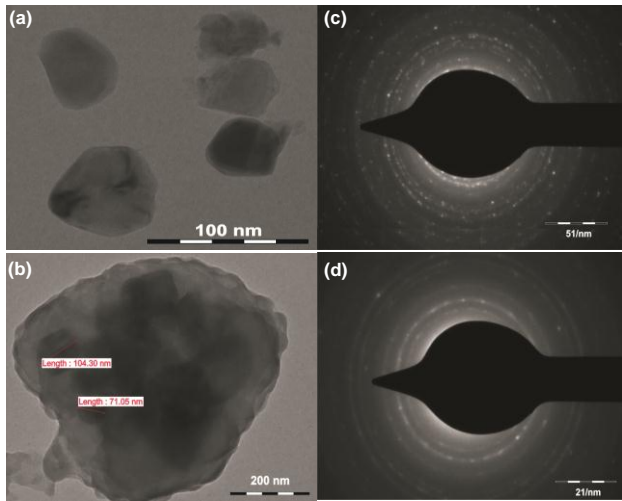
Fig. 2(a): TEM image of NiFe$_2$O$_4$, (b): TEM image of PANI/NiFe$_2$O$_4$ (30%), (c): SAED pattern of NiFe$_2$O$_4$ and (d): SAED pattern of PANI/NiFe$_2$O$_4$ (30%).

Fig. 3(a) shows the UV-Visible spectra of pure PANI and PANI/NiFe$_2$O$_4$ nanocomposites. It is seen obviously from curve of PANI, it showed two strong absorptions at around 315 and 640nm respectively. The first band was assigned as π-π* transition and the other were associated with the transition of benzinoid rings into quinoid ring. It was reported that PANI showed two strong absorptions at 320~340 and 600~660 nm respectively [37]. UV-Visible spectra of PANI/NiFe$_2$O$_4$ nanocomposite show two absorption bands in range of 300-350 nm and 600-650 nm. In comparison**,** the peaks of PANI/NiFe$_2$O$_4$ nanocomposites (PNF-10, 20, 30) with pure PANI, nanocomposites shows red shift in formal peak and blue shift in latter peak. The peak of pure polyaniline nanoparticles at 315nm is based on the π-π* transition of the phenyl ring whereas corresponding peaks of nanocomposites are at 325nm, 337nm and 349nm for PANI/NiFe$_2$O$_4$ nanocomposite (PNF-10, 20, 30) respectively while the peak at 640nm of polyaniline nanoparticles is attributed to the transition of benzoid ring to quinoid ring, the corresponding peak in nanocomposites are at 617nm, 622nm, 630nm showing a blue shift of 10 to 30 nm for PANI/NiFe$_2$O$_4$ nanocomposite (PNF-10, 20, 30) respectively. The red and blue shifts indicate there may be some interaction between NiFe$_2$O$_4$ nanoparticles and polyaniline [**38**]. This suggests that PANI has a lower delocalization of electrons in the polymer chains and/or a lower doping level after the interaction with the NiFe$_2$O$_4$ nanoparticles forming nanocomposites.

The valance band or highest occupied molecular orbit (HOMO) and lowest unoccupied molecular orbital band (LUMO) are separated by an energy gap is called band gap which is of fundamental important, because the energy gap determines the electrical conductivity and optical absorption character of the polyaniline. In the present case, the optical band gap of PANI and PANI/NiFe$_2$O$_4$ nanocomposite has been estimated from the absorbance coefficient data as a function of wavelength using Tauc relation as given in equation (2),

$$\alpha h\vartheta = (h\vartheta - E_g)^n \tag{2}$$

where, Eg is optical band gap, α is absorption coefficient and hυ is energy of incident photon. The transition probability index (n) has discrete values such as 1/2, 3/2, 2 depending upon whether the transition is direct or indirect and allowed or forbidden. From these plots, it is observed that optical band gap decreases with respect to the concentration of NiFe$_2$O$_4$ nanoparticles in PANI. Since NiFe$_2$O$_4$ is direct band gap semiconductor. The band gap was determined by extrapolating the linear region of the curve on hυ axis at α = 0. The optical band gap for pure PANI was found to be 2.82eV whereas PANI/NiFe$_2$O$_4$ nanocomposites exhibited the band gap of 2.58eV, 2.52eV, 2.45eV respectively for PNF-10, 20, 30%. The value of optical band gap was found to decrease after doping. Since the optical absorption depends on the short range order in the amorphous state and defect state associated with it, the decrease in the optical band gap in the present system may be due to reduction in the disorder of the system and increase in the density of defect states [**39-40**].
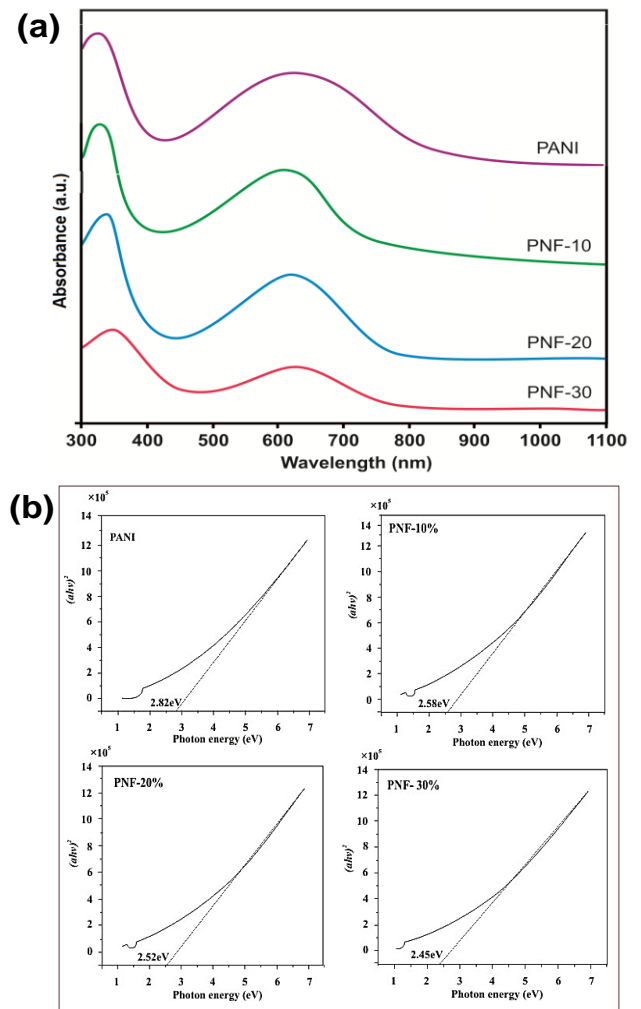
Fig. 3. (a): UV-Visible spectra of pure PANI and PANI/NiFe$_2$O$_4$ nanocomposites, (b) Optical band gap of PANI and PANI/NiFe$_2$O$_4$ nanocomposites.

Conclusion

NiFe$_2$O$_4$ nanoparticles were prepared by reflux method and pure PANI and PANI/NiFe$_2$O$_4$ nanocomposites have been successfully prepared by in-situ chemical oxidization polymerization respectively. XRD result of PANI/NiFe$_2$O$_4$ nanocomposites confirmed that addition of NiFe$_2$O$_4$ content did not change the backbone structure of PANI and shows the peaks of pure ferrites as well as PANI, indicating the uniform mixing of ferrites in PANI. TEM pattern of PANI/NiFe$_2$O$_4$ nanocomposites reflects good interaction between NiFe$_2$O$_4$ nanoparticles and PANI. From UV-Visible spectra of PANI/NiFe$_2$O$_4$ nanocomposites revealed that, as the weight % of NiFe$_2$O$_4$ increases in PANI, the former peaks shows red shift and latter peak shows blue shift which indicates the formation of polaron lattice from extended interaction of semi quinine units. The optical band gap was found to be decreased in case of all nanocomposites compared to pure PANI.

References

1. Malghe, Y. S.; Lavand A.B.; Adv. Mater. Lett. **2016**, 7(3), 239-245.
   DOI: 10.5185/amlett.2016.6130
2. Nabiyouni, G.; Fesharaki, M.J.; Mozafari, M.; Amighian, J.; Chin. Phys. Lett., **2010**, 27, 12, 126401-4.
   DOI: 10.1088/0256-307X/27/12/126401
3. Fesharaki, M.J.; Nabiyouni, G.; Aghamohamadi, M.; Mater. Sci.: Mater. Electron,, **2016**, 27, 4699-4704.
   DOI: 10.1007/s10854-016-4349-0
4. Mosleh, M.; Mater. Sci.: Mater. Electron, **2016**, 27, 6703–6707.
   DOI: 10.1007/s10854-016-4618.
5. Rahman, M. A.; Kumar, P.; Park, D.; Shim, Y.; *Sensor,* **2008**, *8,* 118-141.
   DOI: 10.3390/s8010118
6. Gurunathan, K.; Vadivel, A.; Murugan, Marimuthu, R.; Mulik, U.P.; Amalnerkar, D.P.; *Mater. Chem. Phys.,* **1999**, *61,*173.
   DOI: 10.1016/S0254-0584(99)00081
7. Bidan, G.; Jarjayes, O.; Fruchart, J. M.; Hannecart, E.: Adv. Mater., **1994**, *61*, 152–155.
   DOI: 10.1002/adma.19940060213
8. Kalinina, O.; Kumacheva, F.; Macromol. **1999**, 32, 4122-4129.
   DOI: 10.1021/ma9815830
9. Blinova, N.V.; Stejskal, J.; Trchova, M.; Sapurina, I.; Ciric-Marjanovic, G. Polym., **2009**, 50, 50-56.
   DOI: 10.1016/j.polymer.2008.10.040
10. Li, X.; Gao, Y.; Gong, J.; Zhang, L.; Qu, L.Y.; Phys. Chem. C, **2009**, 113, 69-73.
    DOI: 10.1021/jp807535v
11. Bouazza, S.; Alonzo, V.; Hauchard, D. Synth. Met., **2009**, 159, 1612-1619.
    DOI: 10.1016/j.synthmet.2009.04.025
12. Blinova, N.V.; Bober, P.; Hromadkova, J.; Trchova, M.; Stejskal, J.; Prokes, J.; Polym. Int., **2010**, 59(4), 437-446.
    DOI: 10.1002/pi.2718
13. Krishna, K. R.; Ravinder, D.; Kumar, K.V.; Lincon, Ch.A. World Condens. Matter Phys., **2012**, 2, 153-159.
    DOI: 10.4236/wjcmp.2012.23025
14. Maaz, K.; Karim, S.;, Mumtaz, A.; Magn. Magn. Mater. **2009, 321**(12), 1838-42.
    DOI: 10.1016/j.jmmm.2008.11.098
15. Khairy, M., Gouda, M.E., Adv. Res., **2015**, 6, 555–562.
    DOI: 10.1016/j.jare.2014.01.009
16. Patil, M.; Shrivastav, V.; Appl. Nanosci., **2015**, 5(7), 809-816.
    DOI: 10.1007/s13204-014-0383-5
17. Sharma, R.; Malik, R.; Lamba, S.; Annapoorni, S.; Bull. Mater. Sci., **2008**, 31(3), 409–413.
    DOI: 10.1007/s12034-008-0064-7
18. El-Shishsstawy, R.M., Salam, M.A., Gabal, M.A., and Asiri, A.M., Poly. Comp., **2012**, 33, 532,
    DOI: 10.1002/pc.22186
19. Ziębowicz, B.; Drak M.; Dobrzański, L.A.; *Achiev. Mater. Manuf. Engg.,* **2007**, *191*, 352,
    DOI: 10/1016/j.jmatprotec2007.03.029
20. Parveen, A., Roy, A.S., *Adv. Mat. Lett.* **2013**, *4(9),* 696.
    DOI: 10.5185/amlett.2012.12481
21. Kushwah, B.S.; Upadhaya, S.C.; Shukla, S.; Sikarwar, A.S.; Sengar, R.M.S.; Bhadauria, S. *Adv. Mat. Lett.* **2010**, *2(1),* 43.
    DOI: 10.5185/amlett.2010.8149
22. Nandapure, B.I.; Kondawar, S.B.; Salunkhe, M.Y.; Nandapure, A.I.; *Adv. Mat. Lett.* **2013**, *4(2),* 134.
    DOI: 10.5185/amlett.2012.5348
23. Kargirwar, S.R.; Thakare, S.R.; Choudhary, M.D.; Kondawar, S.B.; Dhakate, S.R.; *Adv. Mat. Lett.* **2011**, *2*, 397.
    DOI: 10.5185/amlett.2011.4245
24. Shukla,S.K.; Bharadvaja, A.; Tiwari, A.; Parashar, G.K.; Dubey, G.C. Adv. Mat. Lett. **2010**, *1(2),* 129-134.
    DOI: 10.5185/amlett.2010.3105
25. Nandapure, A.I.; Kondawar, S.B.; Sawadh, P.S.; Nandapure, B.I. *Phys.B*, **2012**, *407,* 1104-1107.
    DOI: 10.1016/j.physb.2012.01.081
26. Kondawar, S.B.; Dahegaonkar, A.D.; Tabhane,V.A.; Nandanwar, D.V.; Adv. Mat. Lett. **2014**, 5(6), 360-365.
    DOI: 10.5185/amlett.2014.amwc.1036
27. Tan, Y.; Zhang, Y.; Kan,J.; eXPRESS Polym. Lett. **2009**, 3(6), 333-339.
    DOI: 10.3144/expresspolymlett.2009.42
28. Kondawar, S.B.; Deshpande, M.D.; Agrawal, S.P.; Int. Compos. Mater. **2012**, *2(3),* 32.
    DOI: 10.5923/j.cmaterials.20120203.03
29. Song, G.P.; Han, J.; Guo, R.; *Syn. Met.,* **2007**, *157*, 170.
    DOI: 10.1016/j.synthmet.2006.12.007
30. Song, G.P.; Bo, J.; Guo, R.; *Colloid Polym. Sci,* **2005**, *283*, 677.
    DOI: 10.1007/s00396-004-1205-1
31. Rodrigues, A.O.; Ramos, J. M. F.; Gomes, I. T.; Almeida, B. G. ; Araújo, J. P. ; Queiroz, M. R. P.; Coutinho, P. J. G. ; and Castanheira, E. M. S.;*RSC Adv.*, **2016**,6, 17302-17313.
    DOI: 10.1039/C5RA27058H
32. Rodrigues, A.O.; Ramos, J. M. F. ; Gomes, I. T. ; Almeida, B. G. ; Araújo, J. P. ; Queiroz, M. R. P.; Coutinho, P. J. G. ; and Castanheira, E. M. S.; *Phys. Chem. Chem. Phys.*, **2015**,17, 18011.
    DOI: 10.1039/C5CP01894C
33. Shambharkar, B.H.; Umare, S.S.; *Appl. Polym. Sci.*, **2011***, 122*, 1905.
    DOI: 10.1002/app.34286
34. Prasanna G.D.; Prasad V.B.; Jayanna H.S.; Mater. Sci. Eng., **2015,** 73, 012072(1-4).
    DOI: 10.1088/1757-899X/73/1/012072
35. Nandapure, B.I.; Kondawar, S.B.; Nandapure, A.I.; *Adv. Mat. Lett.* **2014**, **5**(6), 339-344.
    DOI: 10.5185/amlett.2014.amwc.1035
36. Lazarevic, Z.Z.; Jovalekic, C.; Milutinovic, A.; Rom£evic, M. J.; Rom£evic, N. Z.; *Acta Phys. Pol.*, **2012***, 121*, 682.
37. PACS numbers: 75.20.-g, 81.07. Wx, 81.20.Ev, 74.25.nd Nandapure, B.I.; Kondawar, S.B.; Salunkhe, M.Y.; Nandapure, A.I.; Compos. Mater. **2013,** *47*, 559.
    DOI: 10.1177/0021998312442559
38. Xia H.; Wang Q.; Chem.Mater. **2002**, 14(5), 2158.
    DOI: 10.1021/cm0109591
39. Reda S.M.; Al-Ghannam S.M.; Adv. Mater. Phys. Chem., **2012,** 2, 75.
    DOI: 10.4236/ampc2012.22013
40. Tiwari, A.; Kobayashi, H. (Eds.); Responsive Materials and Methods; Wiley: USA, **2013**.
    DOI: 10.5185/sbm-2010-01